

Analysis of Microstructures in Traffic Jams on Highways Based on Drone Observations

Yildirim Dülger
Connected Navigation
Daimler AG
Sindelfingen, Germany
yildirim.duelgar@daimler.com

Michael Menth
Computer Science
University of Tübingen
Tübingen, Germany
menth@uni-tuebingen.de

Hubert Rehborn
Connected Navigation
Daimler AG
Sindelfingen, Germany
hubert.rehborn@daimler.com

Micha Koller
Cloud Applications Platform
Daimler AG
Sindelfingen, Germany
micha.koller@daimler.com

Abstract—We investigate vehicle trajectories on a three-lane road segment of a highway which were obtained from drone observations. Based on these comprehensive datasets, we study distance headways to preceding vehicles and develop a method to quantify the local traffic density on a short distance ahead of a vehicle. We leverage these metrics to study a local traffic jam. The new method indicates increased traffic density ahead of a vehicle about 100 meters or 15 seconds before a vehicle is affected by the traffic jam. We also study the connection between vehicle speed and distance headway or traffic density, respectively, and quantify them by conditional probabilities and conditional means. On the one hand, the results give insights into microstructures of traffic jams. On the other hand, the novel method for local density calculation may be applied in vehicles to warn drivers of upcoming high density traffic situations which improves driving safety.

Index Terms—Drone data, traffic density, traffic jam, traffic analysis.

I. INTRODUCTION

One of the main objectives of driver assistance systems and intelligent vehicles is to increase driving safety and decrease or prevent traffic accidents. An important approach is to warn the driver about upcoming traffic events, e.g., an upcoming jam. There are several researches done in the scope of jam warnings (see, e.g., [2]–[4] and references there). The empirical studies about jam warnings mainly use vehicle speeds to detect jam tails. One main reason for only using the speed attribute is the lack of detailed and complete empirical data. E.g., *floating car data (FCD)* only provide GPS-locations of a certain amount of probe vehicles in usually fixed time interval steps which are mostly greater than 3 seconds. The *FCD penetration* rate is the percentage of the vehicles, which are sending their position data, compared to the whole vehicles at a road segment. A FCD penetration rate of 1 – 2% of the whole traffic is a relatively high amount of probe vehicles [2]. In [2] and [3] a method for jam tail warnings is developed using FCD with 5 or 10 second interval steps. Such FCD make it difficult to use other vehicle attributes than the speed, e.g., it is not possible to calculate the distance between consecutive vehicles. Another common data source are induction loop detectors.

This work is supported by the German Federal Ministry of Economic Affairs and Energy in the project *MEC-View* (FKZ: 19A16010B) [1].

They measure all vehicles passing the detectors. Additionally to use the vehicle speeds, it is possible to calculate and use the *traffic flow*, however, only at fixed locations [2], [4]–[7]. The additional attribute traffic flow from induction loop detectors at fixed road locations is a very limited usable vehicle attribute for developing warning systems which should be applicable at all road locations.

One of the main problems of the development of functions for driver assistance systems or intelligent vehicles is the lack of real and complete empirical data of vehicles driving along a stretch of road. This would open opportunities to test the new systems in real-world conditions and scenarios.

Through aerial observations of a road segment very precise measurements of all vehicle trajectories can be done, see Fig. 1. The vehicle position can be measured lane-specific. This is not possible with a *global navigation satellite system (GNSS)*, e.g., the *Global Positioning System (GPS)*, due to the error of GNSS positions which could be up to 15 meters [8], [9]. Furthermore, with aerial observations it is possible to measure following features: *distance headway (DHW)*, which describes the distance between consecutive vehicles at a certain time instant, and the *time headway (THW)*, which describes the time slot between consecutive vehicles passing a certain location. In this study we will focus on DHW. In Fig. 2 DHWs are symbolically marked at a certain time instant. Especially for ADAS (advanced driver assistance systems) and automated vehicles the DHW information could be extremely useful due to the complex traffic dynamics and the limited sensor range. In this paper empirical data gathered

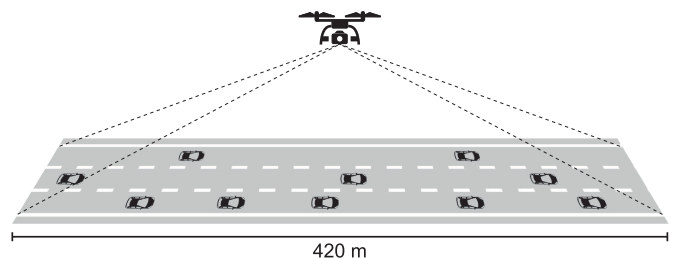


Fig. 1. A drone is recording the highway traffic at an altitude of more than 100 meters. A highway segment with a length of about 420 meters is covered.

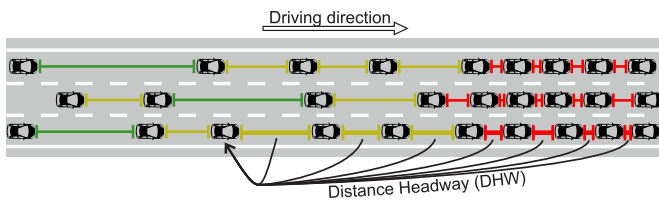


Fig. 2. A frame of the drone recording is symbolically shown from a bird's eye view at a certain time instant. The distance headways (DHWs) between consecutive vehicles are marked by lines between all vehicles in different colors: red for very small DHW, yellow for small DHW and green for little larger DHW. The third down left vehicle on the rightmost lane is symbolically getting the DHW information from the preceding DHWs.

by aerial observations with drones (*unmanned aerial vehicles (UAVs)*) from [10] will be used to investigate DHWs. These datasets were measured during 2017 and 2018 on German highways.

The objective of this paper is the following. Warning systems which warn drivers about upcoming dangerous situations, e.g., jam-tail warning [2], [3], typically use only vehicle speed information. In this paper, we make use of density information consisting of the distances between consecutive vehicles (DHW). Empirical drone measurements on highways from 2017 and 2018 will be used. Based on the density information from this comprehensive datasets, we reveal a new empirical method that uses moving average techniques to warn vehicles in advance about upcoming high densities.

The paper is structured as follows. Section II gives an overview about commonly used data sources. In Section III the empirical data used in this paper are described. Section IV provides an empirical method which warns vehicles about high preceding local densities. Section V concludes this paper.

II. RELATED WORK

Through aerial observations a complete measurement of all vehicle trajectories passing a road segment has been done in 1975 in [11] as well as in the project *Next Generation Simulation (NGSIM)* in 2006 [12]. The NGSIM dataset was measured in the U.S. and includes highways and city traffic. In the years 2017 and 2018 city traffic was investigated by using drones (*unmanned aerial vehicles (UAVs)*) in [13]–[15]. The measured road segment was located at a traffic light in Germany. Most recently, during 2017 and 2018 drone datasets (*highD dataset*) have been recorded in [10] on German highways. In this paper, we study the empirical drone datasets [10].

Empirical traffic investigations have been made since decades with various traffic data sources as floating car data or induction loop detectors (see, e.g., [2], [4] and references there). However, the traffic data sources which have been used do not cover all vehicle trajectories along a stretch of road and are therefore limited.

Through the availability of more detailed traffic data as drone data, more traffic features can be investigated, e.g., distance headways (DHWs) and time headways (THWs) between consecutive vehicles. In [10] and [16] distributions

of DHWs, THWs and vehicle speeds are studied based on empirical data from highways and city traffic. One of the main advantages for vehicles using the DHW and THW information is lane changing. Lane changing dynamics and durations have been studied in [16], [17]. By using empirical traffic data [12] a detailed empirical study about THWs and lane change durations have been done in [16].

Moreover, moving average (MA) methods are used as standard techniques for scientific work, e.g., for smoothing noisy data. In the literature MAs are also known under different terms, e.g., filtering or smoothing methods. There are several studies devoted to unweighted, weighted and exponential moving averages, see, e.g., [18]. A comparison between different moving average methods have been made in [19]. We adapt a MA method to be applicable for non-equidistantly spaced and descending ordered location series.

III. DRONE MEASUREMENTS

In this paper, we make use of empirical drone datasets measured on highways [10] which give a complete spatiotemporal measurement of all vehicle trajectories passing a road segment. Besides vehicle speed information, several more information is given or can be calculated, e.g., distance headways (DHWs) and time headways between consecutive vehicles. We will use the *Highway Drone Dataset (highD dataset)* measured recently during 2017 and 2018 on German highways around Cologne [10]. The dataset includes in total 110 500 different vehicle trajectories, 44 500 driven kilometers and 147 driven hours. The drones recorded at six different highway locations in altitudes of more than 100 meters. At these altitudes the drones are almost not visible for the highway drivers and, therefore, do not influence their driving behavior. Each recording covers a highway segment with a length of about 420 meters as shown in Fig. 1. It was measured at three- and two-lane highway segments. The average recording time is 17 minutes. Different traffic phases are observed in the measurements, e.g., upstream moving jams as observed in Fig. 3 between 8:56 and 8:58 h. Since the most recent computer vision and postprocessing algorithms are used for the drone measurements, the positioning error is relatively small, generally less than ten centimeters [10]. It is a large-scale dataset of high quality which represents the real traffic properly. That is the reason for us to use these datasets to develop our empirical local density method.

In Fig. 3 a drone recording of a length of 19.5 minutes and over a 400 meters highway segment with all vehicle trajectories from the middle lane of a three-lane highway is shown over space and time. We denote the middle lane as lane 2. The vehicle trajectories which are plotted as black lines yield from connecting the vehicle front positions from each frame of the drone recording. It was measured on a German three-lane highway around Cologne at a Monday in October 2017 from 8:55:00 to 9:14:30 h. The corresponding highway infrastructure is shown in Fig. 3 on the right.

Fig. 4 is the subset of Fig. 3 between 100 and 300 meters and between 8:56:00 and 8:58:30 h marked by a dashed square A. The vehicle length of each vehicle is shown in Fig. 4 as

Lane 2 of a highway around Cologne/Germany; Monday, 8:55:00 – 9:14:30 h, October 2017

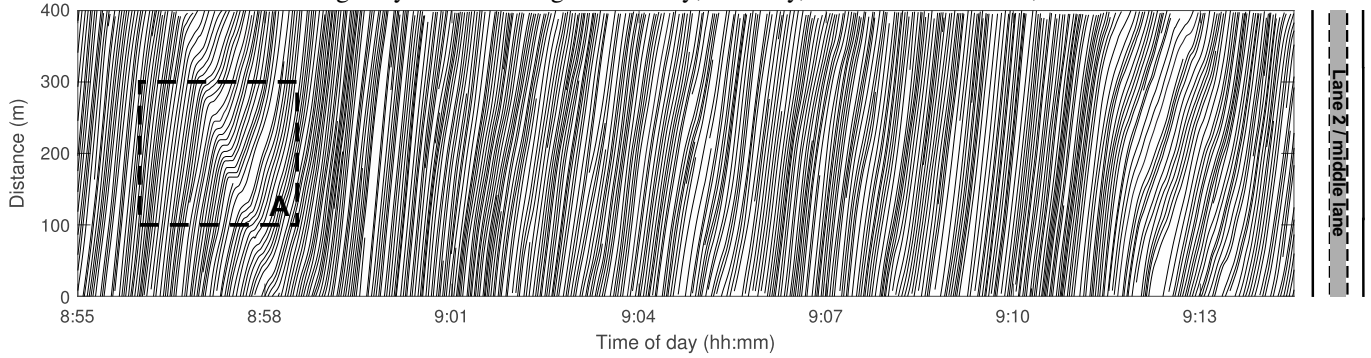


Fig. 3. Microscopic spatiotemporal drone measurement from a German three-lane highway around Cologne at a Monday in October 2017 from 8:55:00 to 9:14:30 h. All vehicle trajectories from the middle lane (lane 2) are shown over space and time. The vehicle trajectories which are plotted as black lines yield from connecting the vehicle front positions from each frame of the drone recording. The corresponding highway infrastructure is shown on the right.

Lane 2; Monday, 8:56:00 – 8:58:30 h, October 2017

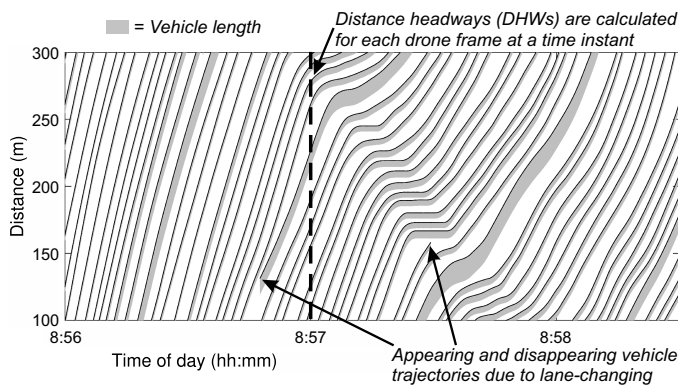


Fig. 4. Microscopic spatiotemporal drone measurement from the middle lane (lane 2) of a German three-lane highway around Cologne at a Monday in October 2017 from 8:56:00 to 8:58:30 h. It is the subset of Fig. 3 marked by a dashed square A. The vehicle length of each vehicle is shown as gray region, whereas the vehicle trajectory that is plotted as black line yield from connecting the vehicle front position from each frame of the drone recording. The corresponding highway infrastructure is shown in Fig. 3 on the right.

gray region along each single trajectory, whereas the vehicle trajectory that is plotted as black line yield from connecting the vehicle front position from each frame of the drone recording. With the vehicle length trucks and large vehicles can be easily identified in Fig. 4, e.g., there is a truck at 8:57:30 h and 100 m. An upstream moving jam can be clearly observed between 8:57 and 8:58 h. Particularly around this upstream moving jam the vehicle density is relatively high. This can be seen by the small DHWs between the consecutive vehicles at the moving jam. Moreover, we see that a large vehicle is changing the lane from one of the other lanes onto lane 2 at around 8:56:45 h and 125 m, whereas at around 8:57:20 h and 150 m another vehicle is changing from lane 2 onto one of the other lanes.

IV. LOCAL TRAFFIC DENSITY

In this section we propose an empirical method that could be used to warn vehicles about local densities. It is based on the

moving average method *UTEMA* [19] and uses the empirical drone measurements [10]. Through the drone measurements complete vehicle trajectories of a road segment over a time interval are given. Therefore, it is possible to calculate the distance headways (DHWs) between consecutive vehicles at each frame of the drone recording. E.g., for the frame at 8:57 h the DHWs are calculated along the vertical dashed line shown in Fig. 4. We aim to apply a moving average technique to the DHWs for each frame of the drone recording. Density information calculated from averaged DHWs is particularly crucial for automated vehicles and ADAS (advanced driving assistance systems). Vehicles which get a high preceding local density information could react automatically or by the driver in adapting the driving behavior.

A. Moving Average Technique Applied to Distance Headways

Since we will apply a moving average method to non-equidistantly spaced samples without a strong bias towards the first measured sample, we have chosen the *unbiased time-exponential moving average (UTEMA)* proposed in [19]. Moving average methods are usually applied to ascending ordered time series. However, we aim to apply UTEMA to descending ordered *location series*. Therefore, an adaptation of UTEMA from [19] is necessary. In Fig. 5 the procedure of the adapted UTEMA applied to location series at a certain time instant is shown. The location series d_0, d_1, d_2, \dots are the vehicle positions from one highway lane measured by drones.

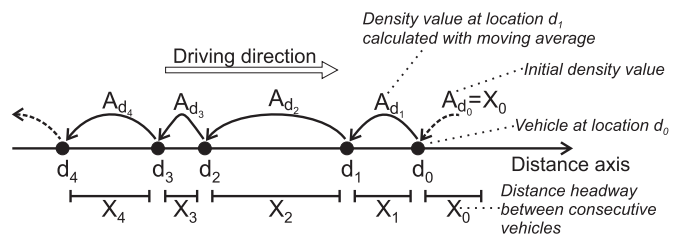


Fig. 5. The procedure of UTEMA applied to location series d_0, d_1, d_2, \dots at a certain time instant is shown. The averages $A_{d_0}, A_{d_1}, A_{d_2}, \dots$ are calculated with UTEMA recursively from (1) – (3).

The averages $A_{d_0}, A_{d_1}, A_{d_2}, \dots$ are calculated with UTEMA. The adapted UTEMA can be calculated recursively from the following equations:

$$S_d = \begin{cases} 0 & d > d_0 \\ X_0 & d = d_0 \\ e^{-\beta \cdot (d_{i-1} - d_i)} \cdot S_{d_{i-1}} + X_i & d = d_i \\ e^{-\beta \cdot (d_i - d)} \cdot S_{d_i} & d_i > d > d_{i+1} \end{cases} \quad (1)$$

$$N_d = \begin{cases} 0 & d > d_0 \\ 1 & d = d_0 \\ e^{-\beta \cdot (d_{i-1} - d_i)} \cdot N_{d_{i-1}} + 1 & d = d_i \\ e^{-\beta \cdot (d_i - d)} \cdot N_{d_i} & d_i > d > d_{i+1} \end{cases} \quad (2)$$

$$A_d = \begin{cases} \frac{S_d}{N_d} & N_d > 0 \\ 0 & N_d \leq 0 \end{cases}, \quad (3)$$

where X_i is the DHW between the two vehicles at the locations d_i and d_{i-1} , A_d is the location-dependent average of DHWs at location d and β is a smoothing parameter, e.g., $\beta = \frac{1}{100}$. We note that for the very first locations the average value A_d uses a small number of X_i . An important metric to characterize moving average properties is the *memory* M . The memory M is basically the space range over which X_0, X_1, X_2, \dots are averaged. For UTEMA it holds

$$M = \frac{1}{\beta}.$$

In Fig. 6 (c) we have used $M = 100$ meters, i.e., $\beta = \frac{1}{100}$.

To apply the local density method described above for a whole drone measurement, we do the following steps:

-
- Step 1: Consider the data from the frame of the drone recording starting with the first one.
 - Step 2: Define the descending ordered location series d_0, d_1, d_2, \dots and calculate all DHWs X_0, X_1, X_2, \dots between consecutive vehicles.
 - Step 3: For each location d_i calculate the average A_{d_i} with UTEMA recursively from (1) – (3) starting at d_0 .
 - Step 4: Take the next frame of the drone recording and start with Step 1 until the last frame is reached.
-

The calculated average value A_{d_i} gives the density information ahead the vehicle's current location d_i . If the density value A_{d_i} is relatively small the vehicle could get a density information, e.g., a warning about high preceding local density. We denote the average values A_{d_i} , which are calculated by applying UTEMA to DHWs, as *UTEMA-DHWs*.

In Fig. 6 (a) – (c) the subset of the drone measurement marked by a dashed square A in Fig. 3 are shown. Fig. 4 shows the same subset. In Fig. 6 (a) the vehicle trajectories are colored according their speeds. In Fig. 6 (b) and (c) the vehicle trajectories are colored according the distance to preceding vehicles (DHWs) and the averaged UTEMA-DHWs, respectively. The colors are chosen for visualization purposes. An upstream moving jam within vehicles have very low speeds can be observed between 8:57 and 8:58 h marked by two dotted black lines in Fig. 6 (a). Furthermore, we see

that the vehicle speeds are higher before entering the moving jam (see orange colored trajectories with speeds between 20 and 35 km/h) than after leaving the moving jam (see red colored trajectories with speeds between 0 and 10 km/h). In Fig. 6 (b) very small DHWs can be observed especially inside the moving jam. However, there are also vehicles with very small DHWs after the moving jam. This occurs, e.g., if a vehicle is driving very close to its preceding vehicle along this highway segment.

In Fig. 6 (c) an interesting observation can be made: a local density front marked by a dotted black line with very low UTEMA-DHW values (0 – 10 m, colored in red). It is moving upstream similar to the moving jam which is marked

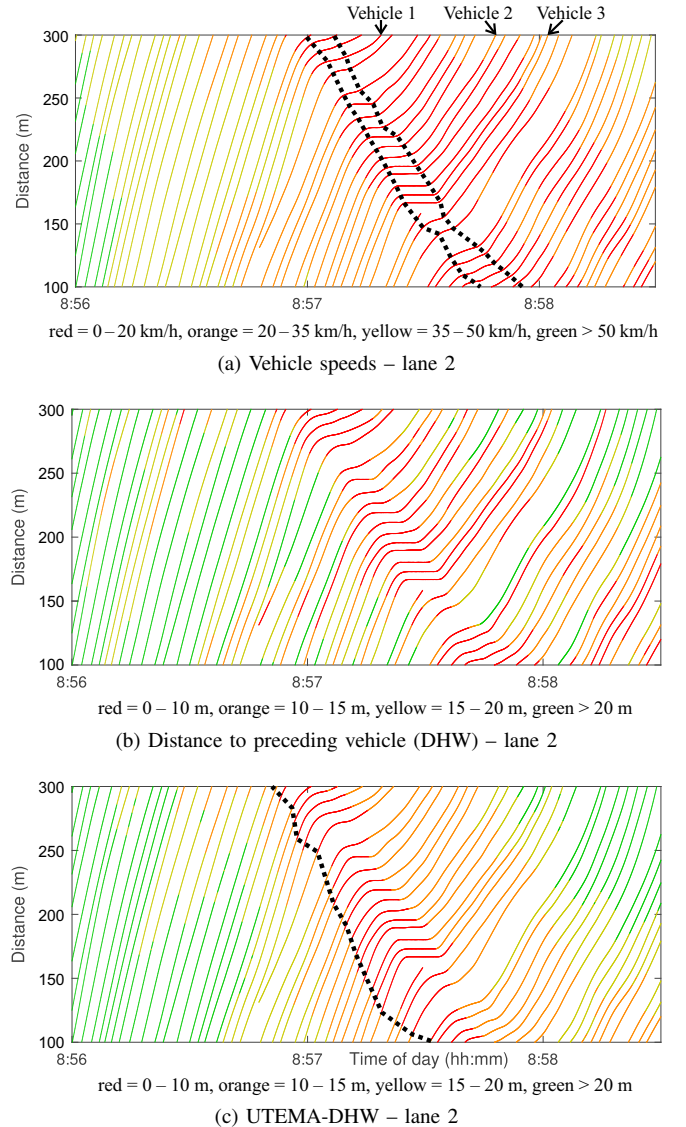


Fig. 6. Vehicle trajectories from the middle lane (lane 2) of a German three-lane highway around Cologne from 8:56:00 to 8:58:30 h are shown in space and time. It is the subset of Fig. 3 marked by a dashed square A and the same data shown in Fig. 4. The vehicle trajectories in (a) are colored according the vehicle speeds, in (b) according the distance to preceding vehicles (DHWs) and in (c) according UTEMA-DHWs.

by two dotted black lines in Fig. 6 (a). Due to the definition of our local density method described above, the density front is in space and time located before the upstream moving jam. In fact, the density front is observed around 100 meters and 15 seconds earlier (Fig. 6 (c)) compared to the density information from the distance headways (DHWs) between consecutive vehicles (Fig. 6 (b)). That means, the vehicles get the high density information (very low UTEMA-DHW values) before they reach the location where it is very dense (very low DHW values). Fig. 7 illustrates this observation with three vehicle trajectories marked in Fig. 6 (a) as Vehicle 1, 2 and 3. DHW and UTEMA-DHW are plotted for all three vehicles over distance in Fig. 7 (a), (c) and (e) and over time in Fig. 7 (b), (d) and (f). The black arrows in Fig. 7 shows that the solid black line (UTEA-DHW) drops earlier to smaller values than the dotted black line (DHW). Therefore, the vehicles get the density information (UTEA-DHW) before they reach the dense region around the moving jam (red marked region in Fig. 6 (b)). Thus, the vehicle could consider the density information in case of small UTEMA-DHWs as a density warning about upcoming high densities. It is important to mention that the location of the density front (dotted black line in Fig. 6 (c)) in space and time depend on the memory M used for the moving average method UTEMA. A larger memory value M would basically increase the space range over which distance headways between consecutive are averaged.

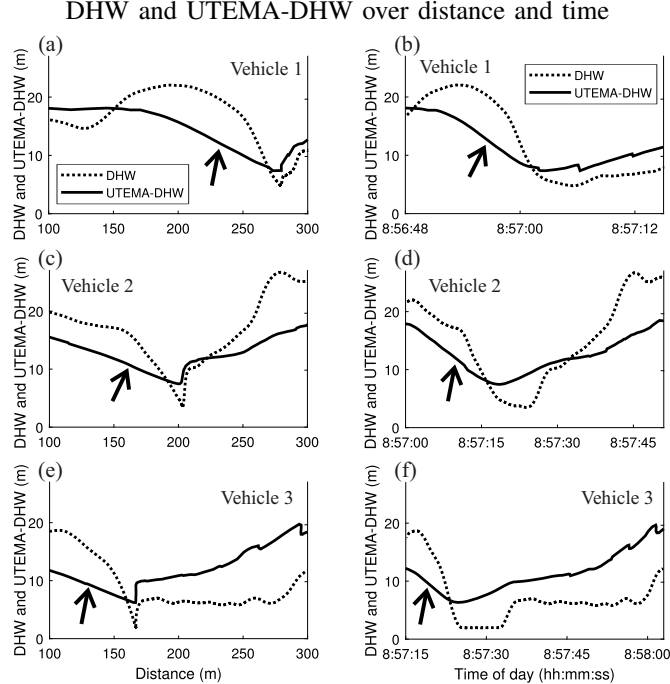


Fig. 7. The vehicle trajectories which are marked in Fig. 6 (a) as vehicle 1, 2 and 3 are shown for the following values: Distance to preceding vehicles (DHWs) (dotted line) and UTEMA-DHWs (solid line). (a) and (b) corresponds to vehicle 1, (c) and (d) to vehicle 2, and (e) and (f) to vehicle 3. The trajectories are plotted in (a), (c) and (e) over the highway distance and in (b), (d) and (f) over time.

B. Conditional Probability Distributions

To study probability distributions we have used several drone measurements from different three-lane highways during different days, including the data used in Fig. 3, Fig. 4 and Fig. 6. In Fig. 8 (a) and (b) probability densities are shown for DHW and UTEMA-DHW, respectively, depending on speed intervals. In Table I the means and medians of DHWs and UTEMA-DHWs depending on speed intervals are listed. The probability density curves in Fig. 8 and the mean and median values in Table I emphasize the known correlation between traffic density and vehicle speed. DHWs and UTEMA-DHWs are increasing with increasing speed intervals. This could be expected because from high speeds it follows that large gaps to preceding vehicles are needed. We quantified this correlations with comprehensive empirical drone data.

V. CONCLUSIONS AND OUTLOOK

Based on drone observations we have revealed an empirical method which uses distances between consecutive vehicles and calculates averaged density values about the traffic ahead the vehicle's current location. A vehicle could use this density information in various ways: (i) As a warning for the driver about upcoming high density. (ii) The vehicle could adapt its driving behavior automatically or by the driver, e.g., by speed adaptation or by increasing the distance to the preceding vehicle. (iii) The driver or the vehicle itself could change the lane to avoid high upcoming traffic density and to reduce the density on its lane.

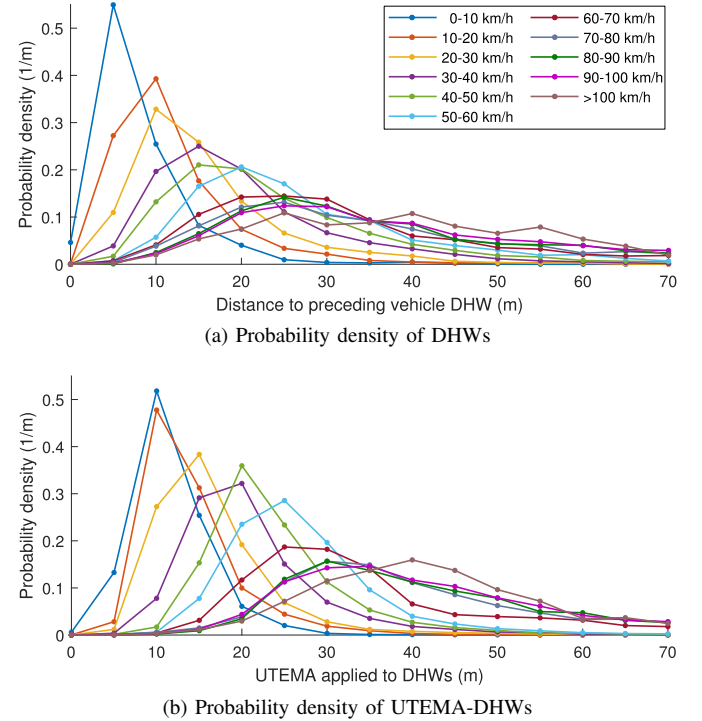


Fig. 8. The probability density for DHWs and for UTEMA-DHWs depending on speed intervals are shown in (a) and (b), respectively. Vehicle data from drone measurements at different lanes, locations and days with different traffic phases are used, including the drone measurement shown in Fig. 3.

TABLE I
MEAN AND MEDIAN OF DHWS AND UTEMA-DHWS DEPENDING ON
SPEED INTERVALS

Speed interval (km/h)	Mean/median of DHW (m)	Mean/median of UTEMA-DHWS (m)
0 – 10	8.4 / 6.6	11.7 / 11.0
10 – 20	12.5 / 10.0	14.3 / 12.4
20 – 30	16.8 / 13.5	17.8 / 15.0
30 – 40	21.1 / 17.8	21.3 / 19.3
40 – 50	24.3 / 20.8	24.3 / 22.1
50 – 60	28.3 / 24.2	27.4 / 25.5
60 – 70	38.1 / 29.6	39.7 / 31.8
70 – 80	43.9 / 33.6	46.7 / 38.4
80 – 90	43.0 / 34.2	45.6 / 39.5
90 – 100	42.8 / 35.8	43.8 / 39.2
> 100	45.3 / 40.6	45.1 / 41.9

The conditional probability distributions which we have done based on empirical drone data have quantified the known dependency between vehicle speed and distance headway between consecutive vehicles (DHW), and between vehicle speed and the density information calculated by our proposed local density method (UTEMA-DHW).

A more detailed quantitative analysis of the density information calculated by our proposed method with a larger amount of data would be interesting. Moreover, the evaluation of the proposed method should be done by performance metrics which have to be defined. These are parts of future work.

The density information which consists of the distances between consecutive vehicles could be measured by existing vehicle distance sensors instead of drone measurements which have been used in this paper. Through vehicle-to-vehicle communication the density information ahead would be available for each vehicle. This is probably a more feasible method to get distances between consecutive vehicles than through drone measurements.

To understand real microscopic traffic features of congested traffic very precise and detailed empirical data is crucial, e.g., drone measurements. We expect from further investigations with these comprehensive traffic data new insights regarding congested traffic features and new contributions to the discussions in traffic theories.

Lane-level vehicle trajectories from drone data have shown that traffic jams and dense regions occur at different locations in space and time. A lane-level investigation of traffic structures would be an interesting task for further studies.

ACKNOWLEDGMENT

We thank the *Institute for Automotive Engineering (ika)* of *RWTH Aachen University* for providing highway drone datasets [10]. We would also like to thank our partners for their support in the project *MEC-View* (FKZ: 19A16010B) [1], funded by the German Federal Ministry of Economic Affairs and Energy.

REFERENCES

- [1] (2017) Mobile edge computing based object detection for automated driving. Accessed December 18, 2018. [Online]. Available: <http://www.mec-view.de>
- [2] B. S. Kerner, H. Rehborn, R.-P. Schäfer, S. L. Klenov, J. Palmer, S. Lorkowski, and N. Witte, "Traffic dynamics in empirical probe vehicle data studied with three-phase theory: Spatiotemporal reconstruction of traffic phases and generation of jam warning messages," *Physica A: Statistical Mechanics and its Applications*, vol. 392, no. 1, pp. 221–251, 2013.
- [3] S.-E. Molzahn, H. Rehborn, and M. Koller, "Jam tail warnings based on vehicle probe data," *Transportation research procedia*, vol. 27, pp. 808–815, 2017.
- [4] B. S. Kerner, *Breakdown in Traffic Networks: Fundamentals of Transportation Science*. Berlin: Springer, 2017.
- [5] M. Treiber and A. Kesting, "Evidence of convective instability in congested traffic flow: A systematic empirical and theoretical investigation," *Procedia-Social and Behavioral Sciences*, vol. 17, pp. 683–701, 2011.
- [6] —, "Calibration and validation of models describing the spatiotemporal evolution of congested traffic patterns," *arXiv preprint arXiv:1008.1639*, 2010.
- [7] Y. Dülger, H. Rehborn, S.-E. Molzahn, M. Koller, M. Menth, B. Kerner, and M. Schreckenberg, "A study for merging of automated vehicles," in *27th Aachen Colloquium Automobile and Engine Technology 2018*, 2018.
- [8] B. Hofmann-Wellenhof, H. Lichtenegger, and J. Collins, *Global positioning system: theory and practice*. Springer Science & Business Media, 2012.
- [9] B. W. Parkinson, P. Enge, P. Axelrad, and J. J. Spilker Jr, *Global positioning system: Theory and applications, Volume II*. American Institute of Aeronautics and Astronautics, 1996.
- [10] R. Krajewski, J. Bock, L. Kloeker, and L. Eckstein, "The highD dataset: A drone dataset of naturalistic vehicle trajectories on german highways for validation of highly automated driving systems," in *2018 IEEE 21st International Conference on Intelligent Transportation Systems (ITSC)*, 2018.
- [11] J. Treiterer, "Investigation of traffic dynamics by aerial photogrammetry techniques," Ohio State University, Columbus, OH United States, final report EES-278 Final Rpt., OHIO-DOT-09-75, FCP 40T2-052, PB 246 094, 1975.
- [12] (2006) NGSIM - Next Generation Simulation. Accessed December 18, 2018. [Online]. Available: <https://ops.fhwa.dot.gov/trafficanalysisstools/ngsim.htm>
- [13] S. Kaufmann, B. S. Kerner, H. Rehborn, M. Koller, and S. L. Klenov, "Aerial observation of inner city traffic and analysis of microscopic data at traffic signals," *Transportation Research Board Annual Meeting*, 2017.
- [14] S. Kaufmann, "Luftbeobachtung und Interpretation mikroskopischer Verkehrsmuster im übersättigten Verkehr vor Lichtsignalanlagen," Ph.D. dissertation, University of Tübingen, Germany, December 2018. [Online]. Available: <http://dx.doi.org/10.15496/publikation-26626>
- [15] S. Kaufmann, B. S. Kerner, H. Rehborn, M. Koller, and S. L. Klenov, "Aerial observations of moving synchronized flow patterns in over-saturated city traffic," *Transportation research part C: emerging technologies*, vol. 86, pp. 393–406, 2018.
- [16] C. Thiemann, M. Treiber, and A. Kesting, "Estimating acceleration and lane-changing dynamics from next generation simulation trajectory data," *Transportation Research Record: Journal of the Transportation Research Board*, no. 2088, pp. 90–101, 2008.
- [17] A. Kesting, M. Treiber, and D. Helbing, "General lane-changing model mobil for car-following models," *Transportation Research Record*, vol. 1999, no. 1, pp. 86–94, 2007.
- [18] E. Zivot and J. Wang, "Vector autoregressive models for multivariate time series," *Modeling Financial Time Series with S-PLUS*, pp. 385–429, 2006.
- [19] M. Menth and F. Hauser, "On moving averages, histograms and time-dependent rates for online measurement," in *8th ACM/SPEC on International Conference on Performance Engineering*. ACM, 2017, pp. 103–114.